

# Inhibitive Action of Aniline on Zinc Corrosion in a H<sub>2</sub>SO<sub>4</sub> Solution: Electrochemical Study

R. T. Vashi<sup>1\*</sup>, S. A. Zele<sup>2</sup> and N. I. Prajapati<sup>1</sup>

<sup>1</sup> *Department of Chemistry, Navyug Science College – Rander Road, Surat, India*

<sup>2</sup> *B. K. M. Science College, Tithal Road, Valsad – 396 001, Gujarat, India*

\*Corresponding author: vashirajendra@yahoo.co.in

Received 24/11/2019; accepted 15/07/2021

<https://doi.org/10.4152/pea.2022400205>

---

## Abstract

Aniline corrosion inhibitor effect on zinc in a H<sub>2</sub>SO<sub>4</sub> solution has been evaluated by weight loss (WL), potentiodynamic polarization (PDP), electrochemical impedance spectroscopy (EIS) and Scanning Electron Microscope (SEM) techniques. The corrosion rate increased with higher acid concentrations. At constant inhibitor content, with higher acid concentrations, the corrosion rate increased. With higher inhibitor concentrations the corrosion rate decreased, while inhibition efficiency (IE) percentage increased. The maximum IE of 90.18% was obtained at 60 mM of aniline in a 0.5 M H<sub>2</sub>SO<sub>4</sub> solution. Polarization studies revealed that aniline acts as a mixed type inhibitor. EIS spectra are semicircular, which indicates that zinc corrosion was mainly controlled by a charge transfer process. SEM reveals the appearance of a smooth surface on zinc in aniline presence, probably due to the formation of an adsorptive film of electrostatic character. It was found that there is a good agreement between the different tested techniques.

**Keywords:** Zinc, H<sub>2</sub>SO<sub>4</sub>, aniline effect, polarization and EIS.

---

## Introduction

Zinc is a metal with numerous industrial applications, and it is mainly used for steel corrosion protection [1]. It is an industrially important metal and it is corroded by many agents, of which aqueous acids are the most dangerous [2]. Corrosion damage generates high cost for inspection, repairing, and replacement; thus, there is a need for using substances that behave like corrosion inhibitors, especially in acidic media [3]. H<sub>2</sub>SO<sub>4</sub> acid is a strong acid, used as a cleaner for rust, algae and scale from condensers and cooling towers [4]. Aromatic, aliphatic and heterocyclic amines compounds comprising oxygen, nitrogen, or sulfur hetero atoms have been extensively investigated as corrosion inhibitors [5]. The corrosion inhibition efficiencies strongly depend on the inhibitor capability to adsorb onto the metal surface, and on the chemical, physical and structural properties of organic molecules [6]. Many researchers [7-18] studied zinc corrosion inhibition in H<sub>2</sub>SO<sub>4</sub> by various organic inhibitors. Various researchers [19-23] studied zinc corrosion in different acidic solutions. Several studies [24-28] used aniline as an inhibitor for zinc corrosion in different acidic media. The aim of the present study is to investigate aniline inhibition effect on zinc corrosion in various concentrations of H<sub>2</sub>SO<sub>4</sub> solutions, by weight loss, polarization, EIS and SEM techniques.

## **Experimental**

### ***Sample and solution preparation***

Zinc specimens, with a chemical composition of 99.39% Zn, 0.49% Mn and 0.12% Co, were used in the present study. Metal sheet test specimens, with a size of 5.0 x 2.5 x 0.2 cm and an effective area of 0.3013 dm<sup>2</sup>, were used. The specimens were cleaned with distilled water, degreased by acetone, washed once more with doubled distilled water, finally dried, and weighted by an electronic balance. H<sub>2</sub>SO<sub>4</sub> was used as a corrosive solution, with concentrations of 0.1, 0.3 and 0.5 M, prepared by diluting analytical grade of H<sub>2</sub>SO<sub>4</sub>, purchased from Merck, using double distilled water.

### ***Weight loss measurements***

For weight-loss measurements, the zinc coupons were each suspended and completely immersed in 230 mL of 0.1, 0.3 and 0.5 M H<sub>2</sub>SO<sub>4</sub> solutions, in the absence and presence of different aniline concentrations, at 301± 1 K, for an immersion period of 24 h. After the test, the specimens were cleaned by using a 10% chromic acid solution with 0.2% BaCO<sub>3</sub> [29]. After cleaning, test specimens were washed with double distilled water, followed by acetone, dried with an air drier and reweight. From the weight loss data, corrosion rate (CR) was calculated.

### ***Potentiodynamic polarization measurements***

For the polarization study, zinc specimens with an area of 1 cm<sup>2</sup> were immersed in 230 mL 0.1 M H<sub>2</sub>SO<sub>4</sub>, in aniline absence and presence. The test cell (CH instruments, Inc., USA) included the metal specimens as a working electrode, Ag/AgCl as a reference electrode and platinum as an auxiliary electrode. Before each electrochemical measurement, the working electrode was allowed to stand for 50 min in the test solutions, to establish a steady-state open circuit potential (OCP). Polarization curves were plotted with the potential against log current density (called Tafel plots). Cathodic and anodic polarization curves gave cathodic and anodic Tafel lines, correspondingly. The intersect point of cathodic and anodic Tafel lines gave the corrosion current (I<sub>corr</sub>) and the corrosion potential (E<sub>corr</sub>) [30]. Cathodic Tafel slope (β<sub>c</sub>) and anodic Tafel slope (β<sub>a</sub>) were calculated from the software installed in the instrument.

### ***Electrochemical Impedance Spectroscopy (EIS) measurements***

EIS measurements were made (using CH instruments, Inc., USA) at corrosion potentials over a frequency range from 1 KHz to 100 KHz, by a sine wave with a potential perturbation amplitude of 5 mV. The real Z' and imaginary -Z'' parts were measured at various frequencies. A graph was drawn by plotting real impedance (Z') versus imaginary impedance (-Z''). From the Nyquist plots of Z' vs Z'', the charge transfer resistance (R<sub>ct</sub>) and double layer capacitance (C<sub>dl</sub>) were calculated. An experiment was carried out in the inhibitor absence and presence.

### ***Scanning electron microscope (SEM) study***

The zinc specimens were immersed in 0.1 M H<sub>2</sub>SO<sub>4</sub> without inhibitor (blank) and with 60 mM of aniline, for one day, at 301 K. After exposure, the specimens were

removed, rinsed with double distilled water, dried and observed in a scanning electron microscope to examine their surface morphology. SEM images of polished zinc specimens were also taken. The surface morphology measurements of zinc specimens were examined using a JEOL-5610 LV (Made in Japan) computer controlled SEM.

## Result and discussion

### Weight loss experiments

The weight loss experiments were carried out in 0.1, 0.3 and 0.5 M H<sub>2</sub>SO<sub>4</sub> solutions with 30, 40, 50 and 60 mM aniline, at 301±1 K, for an exposure period of 24 h.

Inhibition efficiency (I.E) was calculated by using the following equation:

$$IE (\%) = \left\{ \frac{(W_u - W_i)}{W_u} \right\} \times 100 \quad (1)$$

where  $W_u$  is the weight loss in the inhibitor absence and  $W_i$  is the weight loss in the inhibitor presence.

### Acid concentration effect

Results showed in Table 1 indicate that, with higher acid concentrations, the corrosion rate increased. The corrosion rates were 1035.50, 2880.84 and 6179.88 mg/dm<sup>2</sup>.d, corresponding to 0.1, 0.3 and 0.5 M H<sub>2</sub>SO<sub>4</sub> concentrations, respectively, for an immersion period of 24 h, at 301± 1 K. This observation is in agreement with previous works that have been reported [24-28]. The increased corrosion rate with the rise in acid concentrations may be due to an increase in the proton acid (H<sup>+</sup>) transportation action to the zinc surface, so that the reduction reaction at the cathode in the microscopic corrosion cells is enhanced in the inhibitor absence.

### Inhibitor concentration effect

At constant acid content, with higher inhibitor concentrations, the corrosion rate decreased, while IE increased. In 0.5 M H<sub>2</sub>SO<sub>4</sub>, aniline shows an IE of 67.80, 69.06, 76.48 and 90.18%, which corresponds to 30, 40, 50 and 60 mM inhibitor concentrations, respectively (Table 1). This observation is in agreement with previous work that have been reported [24-28].

**Table 1.** H<sub>2</sub>SO<sub>4</sub> concentration effect on zinc C. R. and aniline inhibition efficiency (IE), with various concentrations.

Inhibitor concentration (mM)	Acid concentration					
	0.01 M		0.03 M		0.05 M	
	CR (mg/dm <sup>2</sup> d)	IE (%)	CR (mg/dm <sup>2</sup> d)	IE (%)	CR (mg/dm <sup>2</sup> d)	IE (%)
Blank	1035.50	--	2880.84	--	6179.88	--
30	710.56	31.38	1635.16	43.24	1989.92	67.80
40	464.83	55.11	1039.40	63.92	1912.05	69.06
50	328.77	68.25	742.10	74.24	1453.50	76.48
60	167.85	83.82	337.92	88.27	606.86	90.18

**Potentiodynamic polarization study**

Fig. 1(a) and Fig. 1(b) represent the potentiodynamic polarization curves for zinc in 0.1 M H<sub>2</sub>SO<sub>4</sub>, without and with 60 mM aniline, respectively.

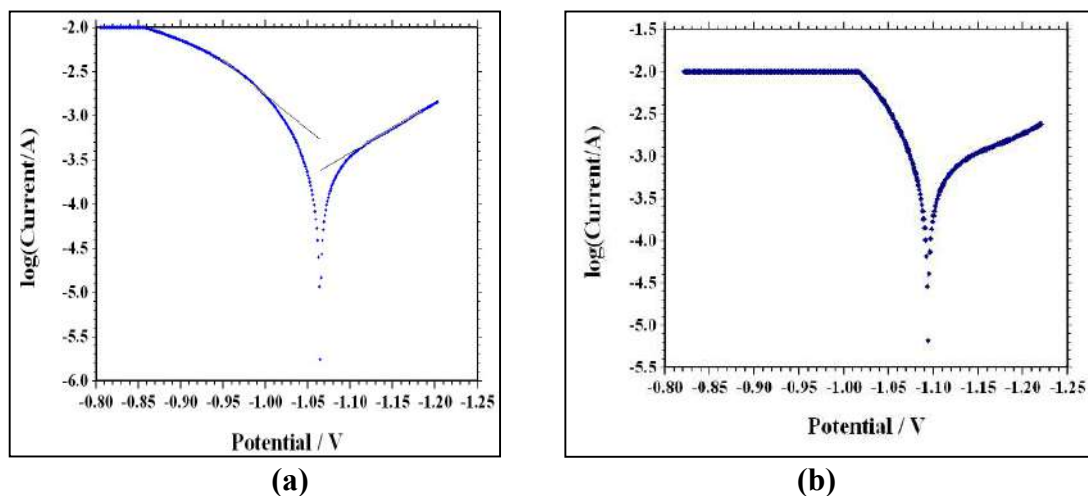


**Figure 1.** Tafel polarization curves (a) for Zinc in 0.1 M H<sub>2</sub>SO<sub>4</sub> without inhibitor and (b) with 60 mM aniline.

Electrochemical parameters, such as  $E_{\text{corr}}$ ,  $I_{\text{corr}}$ ,  $\beta_a$ ,  $\beta_c$ ,  $\beta$ , Tafel constant and IE percentage are given in Table 2.

**Table 2.** Potentiodynamic polarization data and aniline IE for zinc corrosion in 0.1 M H<sub>2</sub>SO<sub>4</sub>, at 301 K.

System	$E_{\text{corr}}$ (mV)	$I_{\text{corr}}$ ( $\mu\text{A}/\text{cm}^2$ )	Tafel slope (mV/decade)		Tafel constant ( $\beta$ ) (mV)	IE(%) from methods by weight polarization loss	
			Anodic ( $+\beta_a$ )	Cathodic ( $-\beta_c$ )			
Blank	-1094	2.2320	413.3	219.1	62.2	--	--
Aniline	-1065	0.2284	127.8	176.0	32.2	83.97	89.76

IE from the polarization study was calculated using the following equation [31]:

$$\text{I. E. (\%)} = \frac{i_{\text{corr}(\text{unin})} - i_{\text{corr}(\text{inh})}}{i_{\text{corr}(\text{uninh})}} \times 100 \quad (2)$$

where  $i_{\text{corr}(\text{uninh})}$  and  $i_{\text{corr}(\text{inh})}$  are the corrosion current density for the uninhibited acid and inhibited acid, respectively.  $I_{\text{corr}}$  was determined from Tafel extrapolation and linear polarization resistance measurements. It can be seen from polarization curves that they moved towards a lower current density region, in the inhibitor presence. It can also be noted that both anodic and cathodic curves shifted towards lower current densities in the inhibitor presence, without much change in  $E_{\text{corr}}$  values. This finding suggests that investigated aniline inhibits zinc corrosion in an acidic solution by forming a surface film, without changing zinc corrosion mechanism. Here, the inhibiting action can be explained by a simple obstruction of the metal surface active site. In other words, the corroded area reduction is carried out by the surface covering by adsorbed organic molecules. From Table 2, it is observed that aniline addition to the acidic solution causes significant decrease in the corrosion current density ( $I_{\text{corr}}$ ) and a corrosion rate lower than that of the

blank. In general, an inhibitor is anodic or cathodic if the variation in  $E_{\text{corr}}$  against the blank is higher than or above 85 mV [32]. In the present study, the  $E_{\text{corr}}$  displacement was 29 mV (Table 2), which suggests that aniline functions as a mixed type of inhibitor, at 301 K, probably due to the heteroatom (N-atom) electron density. Inhibition efficiencies calculated from the corrosion current obtained by the extrapolation of the cathodic and anodic Tafel lines are given in Table 2. IE from Tafel plots agree well (within  $\pm 6\%$ ) with the values obtained from weight loss data.

### **Electrochemical Impedance Spectroscopy (EIS) measurements**

EIS is a useful tool for studying the electrode surface behavior and predicting the corrosion rate. Nyquist plots, for zinc corrosion in a 0.1 M  $\text{H}_2\text{SO}_4$  solution without and with aniline, were examined by the EIS method, at room temperature, as shown in Fig. 2a and Fig. 2b. EIS parameters are shown in Table 3. The capacitive loop diameter in the inhibitor presence is larger than that in the inhibitor absence. The high frequency capacitive loop is related to  $R_{\text{ct}}$ . To calculate  $C_{\text{dl}}$ , the frequency at which the imaginary component of the impedance is maximum was found as presented in the following equation [33]:

$$C_{\text{dl}} = \frac{1}{2\pi F_{\text{max}} R_{\text{ct}}} \quad (3)$$

where  $F$  is the frequency at the maximum height of the semicircle on the imaginary axis [34].

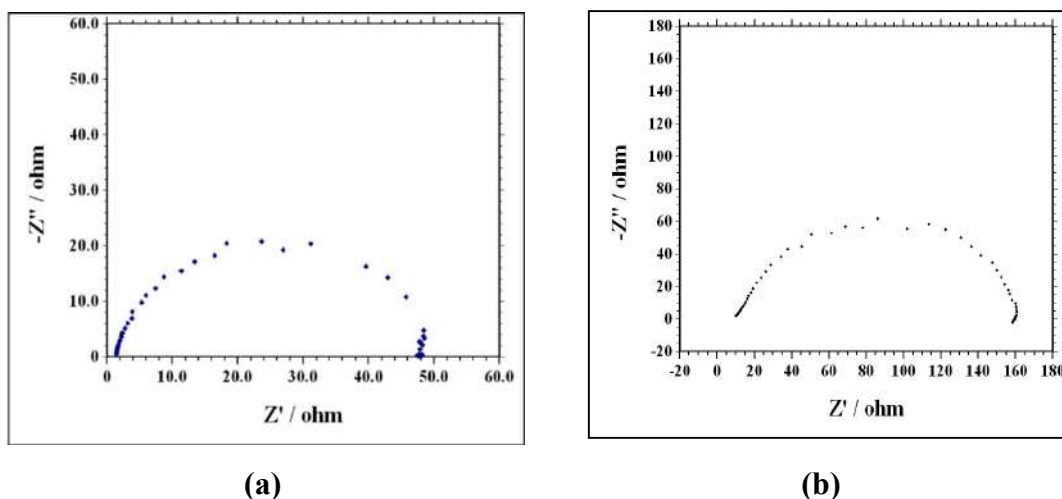


**Figure 2.** Nyquist plots for zinc corrosion in 0.1 M  $\text{H}_2\text{SO}_4$  (a) without inhibitor and (b) with 60 mM of aniline.

**Table 3.** EIS parameters for zinc corrosion in 0.1 M  $\text{H}_2\text{SO}_4$  without and with 60 mM of aniline.

System	$R_{\text{ct}}$ ( $\Omega/\text{cm}^2$ )	$C_{\text{dl}}$ ( $\mu\text{F}/\text{cm}^2$ )	IE(%) from methods by	
			EIS	Weight loss
Blank	49.5	151.84	--	--
Aniline	150.0	16.58	89.08	93.97

IE from the EIS method was calculated using the following equation:

$$IE (\%) = \frac{C_{dl}(\text{uninhi.}) - C_{dl}(\text{inhi.})}{C_{dl}(\text{uninhi.})} \times 100 \quad (4)$$

where  $C_{dl}(\text{uninhi.})$  and  $C_{dl}(\text{inhi.})$  are the double layer capacitance for the uninhibited and inhibited acid, respectively. The inhibitor addition increases  $R_{ct}$  values from 49.5 to 150.0  $\Omega \text{ cm}^2$ , and decreases the  $C_{dl}$  values from 151.84 to 16.58  $\mu\text{F}/\text{cm}^2$ , which is due to the inhibitor adsorption onto the metal surface. The increase in  $R_{ct}$  values was caused by the gradual replacement of water molecules by the inhibitor molecules adsorbed onto the metal surface, forming an adherent film that reduces the extent of dissolution [35]. Moreover, the adsorbed inhibitor species decrease the electrical double layer values at the electrode/solution interface, and, therefore reduce the  $C_{dl}$  value [36]. It was observed from Fig. 3(a) and Fig. 3(b) that the impedance diagram was an imperfect semicircle. The difference has been attributed to frequency dispersion [37]. The semicircle nature of the plots indicates that zinc corrosion was mainly controlled by the charge transfer process.

### **Scanning electron microscope (SEM) measurements**

To understand the surface conditions of the metal specimens, in the inhibitor absence and presence, SEM images were taken. The SEM images are shown in Fig. 3a-c. The SEM image of the freshly polished MS (Fig. 3a) shows a smooth surface, whereas in the 0.1 M  $\text{H}_2\text{SO}_4$  medium (Fig. 3b) it shows a heterogeneous surface with large pits, which indicates that the metal underwent pitting corrosion in the  $\text{H}_2\text{SO}_4$  medium [38]. In contrast, zinc SEM image, after the addition of 60 mM aniline to the 0.1 M  $\text{H}_2\text{SO}_4$  medium, showed a decrease in the number of pits and an increase in the surface smoothness (Fig. 3c).

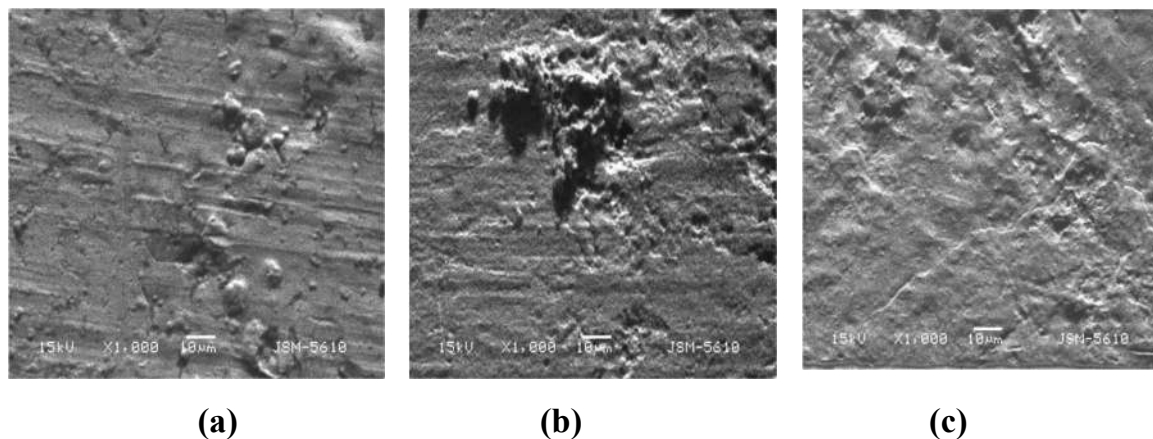


**Figure 3.** Zinc surface SEM images: (a) of polished zinc (b) of zinc immersed in 0.1 M  $\text{H}_2\text{SO}_4$  and (c) of zinc immersed in 0.1 M  $\text{H}_2\text{SO}_4$  with 60 mM aniline (X 1000).

### **Mechanism of inhibition by aniline**

The corrosion inhibitor mechanism is believed to be due to the formation and maintenance of a protective film on the metal surface. Aniline is a weaker base than the primary aliphatic amines, due to resonance, which is not possible in aliphatic amines. Aniline resonance structure is shown in Fig. 4.

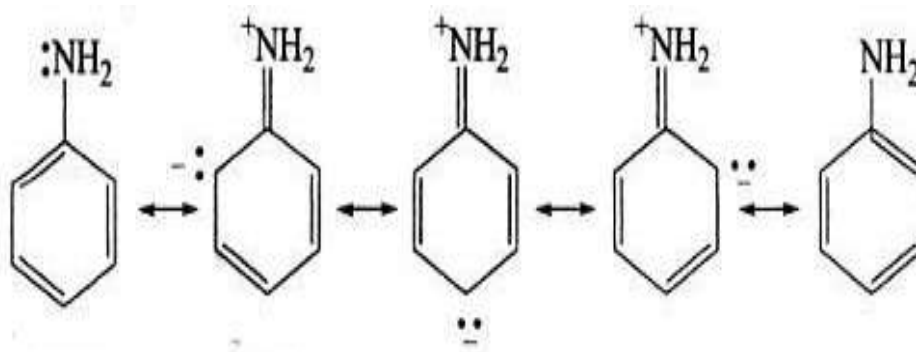


**Figure 4.** Aniline resonance structure.

Due to resonance, in aniline, the lone pair of electrons on the nitrogen atom is less available for coordination with a proton than that in aliphatic amines, where the resonance phenomenon is not possible. In addition to this, the small positive charge on the aniline N-atom, due to resonance, tends to repel the proton. Thus, aniline becomes less basic [39] and, on accepting a proton, may produce a small concentration of the  $C_6H_5^+NH_3$  cation (onium) which does not show resonance. As there are more resonating structures possible for aniline than for the onium ion, the former will be stabilized with respect to the latter [40]. It appears that the amino group nitrogen atom ( $-NH_2$ ) in aniline acts as the reaction center (polar function), because of its higher electron density. This reaction center forms a monolayer on the zinc surface. Moreover, aniline assumes a small positive charge in acidic solutions, due to the amino ( $-NH_2$ ) group protonation, as the higher electron density of the nitrogen atom facilitates the protonation. With higher inhibitor concentrations, the protonation rate increases. The successive increase in protonation may be responsible, in many cases, for the IE enhancement.

## Conclusions

From this study, the following conclusions can be drawn:

1. With higher acid concentrations, the corrosion rate increases.
2. At constant acid concentrations, with higher inhibitor concentrations, the corrosion rate decreases, while IE increases.
3. Maximum IE of 90.18% was obtained with 60 Mm aniline concentration in 0.5 M  $H_2SO_4$ .
4. Polarization curves indicate that aniline act as mixed type of inhibitor.
5. SEM reveals the formation of a smooth surface on zinc, in aniline presence, probably due to the formation of an adsorptive film of electrostatic character.
6. EIS spectra are semicircular in appearance which indicates that zinc corrosion is mainly controlled by a charge transfer process.
7. It was found that there is a good agreement between the different tested techniques.

## Acknowledgement

The authors are thankful to the Department of Chemistry, Navyug Science College, Surat, for providing laboratory facilities.

### Authors' contribution

**R. T. Vashi:** this paper is a part of the Ph. D. Thesis of his student S. A. Zele and he has had guided him for the preparation of this article. **S. A. Zele:** conceived and designed the analysis; prepared and designed this paper under the guidance of co-author Dr. R.T. Vashi; collected all the experimental and other data which are presented in this paper; gave the analytical instruments detailed in the text of this paper; performed all the analyses presented in this paper; wrote this paper. **N. I. Prajapati:** provided support and help in the preparation of the paper of S. A. Zele.

### References

1. Garcia G, Cavellaro L, Broussalis A, et al. Antiviral activity of *Achyroclineflaccida* Wein DC aqueous extract. *Phytother Res.* 1995;9:251-254. Doi: <https://doi.org/10.1002/ptr.2650090404>
2. Manov S, Noli F, Lamazouere AM, et al. Surface treatment for zinc corrosion protection by a new organic chelating reagent. *J App Electrochem.* 1999;29(8):995-1003. Doi: <https://doi.org/10.1023/A:1003585816876>
3. Singh AK. Inhibition of mild steel corrosion in hydrochloric acid solution by 3-(4-((z)-Inddolin- 3-ylideneamino) phenylimino) Indolin-2-one. *Ind Eng Chem Res.* 2012;51(8):3215-3223. Doi: <https://doi.org/10.1021/ie2020476>
4. Sax NI, Lewis RJ. Sr. (eds.). *Hawley's Condensed Chemical Dictionary*, 11th edition, New York, Van Nostrand Reinhold Co., 1987.
5. Hackerman N, Sudbery JD. The effect of amines on the electrode potential of mild steel in tap water and acid solutions. *J Electrochem Soc.* 1950;97:109.
6. Wang H, Liu R, Xin IJ. Inhibition effects of some mercapto-triazole derivatives on the corrosion of mild steel in 1.0 M HCl medium. *Corros Sci.* 2004;46(10):2455-2466. Doi: <https://doi.org/10.1016/j.corsci.2004.01.023>
7. Agrawal YK, Talati JD, Shah MD, et al. Schiff bases of ethylenediamine as corrosion inhibitors of zinc in sulphuric acid. *Corros Sci.* 2004;46:633-651. Doi: [https://doi.org/10.1016/S0010-938X\(03\)00174-4](https://doi.org/10.1016/S0010-938X(03)00174-4)
8. Eddy NO, Odoemelam SA, Ogoko E, et al. Adsorption and inhibitive properties of Lincomycin for the corrosion of zinc in 0.01-0.05 M H<sub>2</sub>SO<sub>4</sub>. *Port Electrochim Acta.* 2009;28:73-85. Doi: <https://doi.org/10.4152/pea.201002073>
9. Fouda AS, Nazeer AA, Ahmed Saber A. Electrochemical Adsorption Properties and Inhibition of Zinc Corrosion by Two Chromones in Sulfuric Acid Solutions. *J Korean Chem Soc.* 2014;58(2):160-168. Doi: <https://doi.org/10.5012/jkcs.2014.58.2.160>
10. Vashi RT, Zele SA, Patel BB. O-Toluidine as Corrosion Inhibitor for Zinc in Sulphuric acid Medium. *Int J Innovative Res in Sci Eng and Tech.* 2019;8(1):559-570.
11. Desai MN, Talati JD, Vyas CV, et al. Some Schiff bases as corrosion inhibitors for zinc in sulphuric acid. *Ind J Chem Technol.* 2008;15:228-237.
12. Vashi RT, Zele SA, Patel BB. Inhibitive action of p-Toluidine on corrosion of zinc in H<sub>2</sub>SO<sub>4</sub> medium. *J Applic Chem.* 2020;9(1):135-145.



13. Vashi RT, Zele SA, Prajapati NI. Aniline as Corrosion Inhibitor for Zinc in H<sub>2</sub>SO<sub>4</sub> Solutions: Kinetic, Adsorption and Thermodynamic Considerations. *Int J Green and Herbal Chem Sec A*. 2020;9(1):034-044. Doi: <https://doi.org/10.24214/IJGHC/GC//9/1/03444>
14. Zele SA, Vashi. RT. Inhibition of corrosion of zinc in sulphuric acid by ethylamines. *Int J Chem Studies*. 2016;4(5):31-38.
15. Zele SA, Patel KK, Vashi RT. Ethanolamines as corrosion inhibitors for zinc in sulphuric acid. *J Appl Chem*. 2017;6(3):350-362.
16. Vashi RT, Zele SA, Patel BB. Inhibitory Properties of N, N-Diethylaniline for Zinc in H<sub>2</sub>SO<sub>4</sub> solutions. *Int J Green and Herbal Chem Sec A*. 2019;(2):525538. Doi: <https://doi.org/10.24214/IJGHC/GC/8/2/52538>
17. Ogoko E, Odoemela SA, Ita B, et al. Adsorption and inhibitive properties of Clarithromycin for the corrosion of Zn in 0.01-0.05 M H<sub>2</sub>SO<sub>4</sub>. *Port Electrochim Acta*. 2008;27(6):713-724. Doi: <https://doi.org/10.4152/pea.200906713>
18. Onwu FK, Ogueji C, Mgbemena NM. Inhibition of Corrosion of Zinc in H<sub>2</sub>SO<sub>4</sub> Medium by the Schiff Base, 4-Hydroxy Phenyl Methylidene-2-(1-Phenyl Ethylidene) Hydrazine Carbothioamide (4-HPMHC). *Der Chemica Sinica*. 2016;7(4):13-20.
19. Saleh KA, Khalil SK. Corrosion inhibition study of zinc in 0.1 M HNO<sub>3</sub> by diphenyl carbazide and caffeine. *Phys Chem Indian J*. 2015;10(1):32-40.
20. Boulkroune M, Chibani A. 2-Thiophene carboxaldehyde as corrosion inhibitor for zinc in phosphoric acid solution. *Chem Sci Trans*. 2012;1(2):355-364. Doi: <https://doi.org/10.7598/cst2012.4730>
21. Vashi RT, Naik D. Inhibiting Properties of Hexamine as Corrosion Inhibitor for Zinc in H<sub>3</sub>PO<sub>4</sub> Solutions: Kinetic, Adsorption and Synergic Effect Study. *Int J for Res in Appl Sci & Eng Tech*. 2021;9(3):1320-1326.
22. Wang L, Xin PJ, Luo H. Corrosion inhibition of zinc in phosphoric acid solution by 2- mercapto benzimidazole. *Corros Sci*. 2003;45(4):677-683. Doi: [https://doi.org/10.1016/S0010-938X\(02\)00145-2](https://doi.org/10.1016/S0010-938X(02)00145-2)
23. Fouda AS, Abdallah M, Atwa ST, et al. Tetrahydrocarbazole derivatives as corrosion inhibitors for zinc in HCl solution. *Modern Appl Sci*. 2010;4(12):41-55. Doi: <https://doi.org/10.5539/mas.v4n12p41>
24. Vashi RT, Bhajiwala HM, Rathod KN. Aniline as corrosion inhibitor for zinc in (HNO<sub>3</sub> + HCl) binary acid mixture. *J Fund and Appl Sci*. 2015;7(2):299-306. Doi: <https://doi.org/10.4314/jfas.v7i2.10>
25. Vashi RT, Desai K. Aniline as corrosion inhibitor for zinc in hydrochloric acid. *Chem Sci Trans*. 2013;2(2):670-676. Doi: <https://doi.org/10.7598.cst2013.423>
26. Vashi RT, Desai SA. Aniline as corrosion inhibitor for zinc in nitric acid. *Multidisciplinary Edu Global Quest*. 2013;2(2):1-8.
27. Vashi RT, Bhajiwala HM, Desai SA. Aniline as corrosion inhibitor for zinc in (HNO<sub>3</sub>+ H<sub>3</sub>PO<sub>4</sub>) binary acid mixture. *Der Pharma Chemica*. 2011;3(2):80-87.
28. Vashi RT, Naik. D. Aniline as corrosion inhibitor for zinc in phosphoric acid. *Int J Chem Tech Res*. 2011;3(2):864-869.

29. Stroud EG. The quantitative removal of corrosion product from zinc. *J Appl Chem.* 1951;1:93-95. Doi: <https://doi.org/10.1002/jctb.5010010301>
30. El Etre AY, Abdallah M, El-Tantawy ZE. Corrosion inhibition of some metal using *Lawsonia* extract. *Corros Sci.* 2005;47(2):385-395. Doi: <https://doi.org/10.1016/j.corosci.2004.06.006>
31. Shah AM, Rahim AA, Hamid SA, et al. Green inhibitors for copper corrosion by Mangrove tannin. *Int J Electrochem Sci.* 2013;8:2140-2153.
32. Li W, Zhao X, Liu F, et al. Investigation on inhibition behaviour of S- triazole-derivatives in acidic solution. *Corros Sci.* 2008;50:3261-3266. Doi: <https://doi.org/10.1016/j.corosci.2008.08.015>
33. Khamis E, Ameer MA, Al-Andis NM, et al. Effect of thiosemicarbazones on corrosion of steel in phosphoric acid produced by wet process. *Corrosion.* 2000;56:27(2):127-138. Doi: <https://doi.org/10.5006/1.3280528>
34. Souza CAC, May JE, Machado AT, et al. Preparation of Fe–Cr–P–Co amorphous alloys by electrodeposition. *Surf Coat Tech.* 2005;190(1):75-82. Doi: <https://doi.org/10.1016/j.surfcoat.2004.04.070>
35. Muralidharan S, Phani KLN, Pitchumani S, et al. Polyamino-benzoquinone polymers - a new class of corrosion-inhibitors for mild-steel. *J Electrochem Soc.* 1995;42(5):1478-1483.
36. Ansfield F. *Corrosion Mechanism.* Marcel Dekker. New York. 1987;119.
37. Dan WX, Bin X, Yuanpeng L, et al. Corrosion control of copper in 3.5 wt.% NaCl solutions by Domperidone: Experimental and theoretically study. *Corros Sci.* 2014;85:77-86. Doi: <https://doi.org/10.1016/j.corosci.2014.04.002>
38. Mansfeld F, Lin S, Kim K, et al. (1987). Pitting and Surface Modification of SiC/Al. *Corros Sci.* 1987;27:997-1001. Doi: [https://doi.org/10.1016/0010-938X\(87\)90065-5](https://doi.org/10.1016/0010-938X(87)90065-5).
39. Rashwan SM, El-Wahab SA, El-Tanany AZ, et al. Electrochemical behaviour of steel in sulphate and chloride solutions and the inhibition effect of some organic nitrogen compounds. *Bull Electrochem.* 1997;13(12):448-455.
40. Chatwal GR. *Reaction mechanism and Reagents in Organic Chemistry.* 1997;74.